NUCL SCI TECH (2020) 31:36
https://doi.org/10.1007/s41365-020-0748-2

Photon energy response optimization using few-channel spectroscopy dose method for Si-PIN photodetector applied in personal dose equivalent measurements

Ping Huang[1,2] · Shu-Qiong Li[1] · Run-Dong Yang[2] · Yun-Tian Sun[2] · Yong Yang[1] · Wu Gao[3]

Received: 26 November 2019 / Revised: 17 February 2020 / Accepted: 18 February 2020 / Published online: 17 March 2020

Abstract Si-PIN photodetectors having features such as low cost, small size, low weight, low voltage, and low power consumption are widely used as radiation detectors in electronic personal dosimeters (EPDs). The technical parameters of EPDs based on the Si-PIN photodetectors include photon energy response (PER), angular response, inherent error, and dose rate linearity. Among them, PER is a key parameter for evaluation of EPD measurement accuracy. At present, owing to the limitations of volume, power consumption, and EPD cost, the PER is usually corrected by a combination of single-channel counting techniques and filtering material methods. However, the above-mentioned methods have problems such as poor PER and low measurement accuracy. To solve such problems, in this study, a 1024-channel spectrometry system using a Si-PIN photodetector was developed and full-spectrum measurement in the reference radiation fields was conducted for radiation protection. The measurement results using the few-channel spectroscopy dose method showed that the PER could be controlled within ± 14% and ± 2% under the conditions of two and three energy intervals, respectively, with different channel numbers. The PER measured at 0° angle of radiation incidence meets the − 29% to +67% requirements of IEC 61526:2010. Meanwhile, the channel number and counts-to-dose conversion factors formed in the experiment can be integrated into an EPD.

Keywords Electronic personal dosimeter · Si-PIN photodetector · Personal dose equivalent · Photon energy response · Few-channel spectroscopy dose method

1 Introduction

Electronic personal dosimeters (EPDs) based on the Si-PIN photodetectors are widely used in nuclear power, atomic reactors, nuclear medicine, and other radiation workplaces. The EPD functions are mainly associated with the measurement of the personal dose equivalent ($H_p(10)$) at a depth of 10 mm in human tissues [1, 2]. Because the sensitive layer thickness of the Si-PIN photodetectors is about 100 μm, the detection efficiency decreases as the photon energy increases. Although a Si-PIN photodetector has advantages in terms of sensitivity, volume, power consumption, and price, it has a drawback in that the low-energy photon response is higher than the high-energy photon response [3, 4]. This phenomenon affects the measuring accuracy of EPDs under different photon energy conditions [5, 6].

Recently, several methods have been proposed for improving the photon energy response (PER) of Si-PIN photodetectors, such as the filtering material method,

This work was partly supported by the National Key Scientific Instruments to Develop Dedicated Program (Nos. 2013YQ090811 and 2016YFF0103800) and the National Key Research and Development Program (No. 2017YFF0211100).

✉ Ping Huang
zhangyaohp@163.com

[1] National Institute of Measurement and Testing Technology, Chengdu 610021, China

[2] Sichuan Radiation Technology Co., Ltd, Chengdu 610021, China

[3] Institute of Microelectronics, School of Computer S&T, Northwestern Polytechnical University, Xi'an 710072, China

spectroscopy dose $G(E)$ function method, energy fluence method, and few-channel spectroscopy dose method.

First, the filtering material method usually reduces the PER of Si-PIN photodetectors for low-energy photons by adding metal materials such as Cu, Al, and Sn in front of the detector. The type, thickness, and shape of the metal materials can be calculated through Monte Carlo simulation or numerical calculation techniques [7, 8]. The back-end circuits are often realized by utilizing the single-channel counting technique. Owing to the difference between the simulated parameters and the real detector characteristics, the PER using the single-channel counting technique for the measurement of $H_p(10)$ can only be controlled within ± 30%.

Second, the spectroscopy dose method uses the $G(E)$ function to correct the PER [9–13]. The measured spectrum multiplied by the counts-to-dose conversion factors (G (E) function) can be used to obtain the dose value. The technique for solving the G (E) function includes Monte Carlo simulation, numerical calculation, or measurement of the full spectrum in the reference radiation fields. This method is used mainly for calculating the area dose equivalent ($H^*(10)$). When measuring $H^*(10)$ using the spectroscopy dose method, the corrected PER can usually be controlled within ± 10%. However, a high-speed analog-to-digital converter (ADC) and field-programmable gate array (FPGA) are employed for rapid processing of the nuclear pulse signals. The disadvantages of this method include high power consumption, limited size, and high cost. Thus, it is unsuitable for the measurement of $H_p(10)$ in human tissues.

In addition to the third method, it is proposed to solve the energy fluence by using the unfolding spectra technique. The value of $H_p(10)$ is then determined by multiplying the unfolding spectra with the counts-to-dose conversion factors of the energy fluence to air kerma and the air kerma to $H_p(10)$ [13–16]. This method has clear steps, and the measurement accuracy is the same as that of the second method. However, the calculation time is relatively long due to the requirement of matrix calculations for unfolding the measured spectra. Thus, this method is not a conducive application for a microcontroller unit (MCU). Meanwhile, similar to the second method, this method also has limitations in terms of power consumption, cost, and volume.

Finally, the few-channel spectroscopy dose method is a simplified version of the spectroscopy dose method. The value of $H_p(10)$ is obtained by multiplying the count values of a few channels (several energy intervals) with the counts-to-dose conversion factors [17, 18]. At present, the energy intervals and counts-to-dose conversion factors are calculated by using the Monte Carlo simulation technique. It is known from relevant publications that the lower detected energy was 100 keV and the inherent error in the range of 0.3–6.0 MeV after correction with three energy intervals was less than ± 20% [17, 18]. Thus, this method has potential to be used for low-power portable EPDs.

This study proposes a novel method where the filter material method and the few-channel spectroscopy dose method are combined to measure the value of $H_p(10)$ for X and gamma radiation. The experimental results showed that the optimum PER were ± 14% and ± 2%, respectively, in the range of 48 keV to 1.25 MeV under the two and three energy intervals, which meet the international standard (IEC 61526:2010) requirements [19]. This method has the characteristics of low power consumption, low cost, simple structure, easy transplantation, and accurate measurement.

2 Theory and method

2.1 Spectroscopy dose method

The spectroscopy dose method is widely used in the measurement of the area dose equivalent ($H^*(10)$) with the NaI, HPGE, and LrBr3 detectors since it can be used without the need for unfolding [9, 10]. The following procedures briefly introduce the basic principle of the spectroscopy dose method. Because the area dose equivalent and the personal dose equivalent can be obtained by the energy fluence multiplied with the counts-to-dose conversion factors, the measured principles of the two quantities using the $G(E)$ function are the same [10, 17]. The personal dose equivalent conversion coefficient $h(E_0)$ can be expressed for mono-energetic X- or gamma rays with the energy E_0 using a response function $R(E, E_0)$ of a radiation detector and the $G(E)$ function as follows [10]:

$$h(E_0) = \int_{E_{\min}}^{E_{\max}} R(E, E_0) G(E) \mathrm{d}E, \tag{1}$$

where $E_{\min} \le E \le E_{\max}$, $E_{\min} \le E_0 \le E_{\max}$, $E_{\min}$ is the minimum detectable energy and $E_{\max}$ is the maximum detectable energy. $R(E, E_0)$ is the detector response function of the Si-PIN photodetector, which represents an X- or gamma-ray of energy E_0 that deposit energy E into the detector.

The value of $H_p(10)$ can be obtained by multiplying the energy fluence and the personal dose equivalent conversion factors, as shown in Eq. (2).

$$H_p(10) = \sum_k \varphi(E_k) h(E_k)$$

$$= \sum_k \varphi(E_k) \int_{E_{\min}}^{E_{\max}} R(E, E_k) G(E) \mathrm{d}E$$

$$= \int_{E_{\min}}^{E_{\max}} \sum_k \varphi(E_k) R(E, E_k) G(E) \mathrm{d}E$$

$$= \int_{E_{\min}}^{E_{\max}} M_{\mathrm{E}} G_{\mathrm{E}} \mathrm{d}E, \quad (2)$$

where $\varphi(E_k)$ is defined as the energy fluence of energy E_k and M_{E} is the measured spectrum of the Si-PIN photodetector in unit time.

When Eq. (2) is represented by the multichannel spectroscopy method, it becomes a discrete form, as shown in Eq. (3), where i is the channel number, and its range is from one to 1024,

$$H_p(10) = M_1 G_1 + M_2 G_2 + \ldots + M_{1024} G_{1024} = \sum_{i=1}^{1024} M_i G_i. \quad (3)$$

2.2 Few-channel spectroscopy dose method

In terms of volume, power consumption, and cost constraints, the high-speed ADC and FPGA chips cannot be used in the EPDs. In addition, the number of internal counters is usually between one and three because of the hardware resource limitations of the ultra-low-power MCU. Therefore, the energy interval of the few-channel spectroscopy dose method is usually also limited from one to three. Compared with the average distribution of the channel number of the multichannel spectroscopy, the channel number in the few-channel spectroscopy dose method can be anywhere between 1 and 1024. Because the EPD uses an ultra-low-power MCU for the measurement of $H_{\mathrm{p}}(10)$, it has great practical value for the development of the few-channel spectroscopy dose method.

The value of the G function in Eq. (3) can be obtained by the Monte Carlo simulation, the numerical calculation, or by measuring the full spectrum in the reference radiation fields. The purpose of this study is to obtain the corresponding channel number and the G value under the optimal PER. Instead of using the Monte Carlo simulation or the numerical calculation to calculate the G value, the enumeration algorithm will be adopted to find the optimal solution because the spectral data processing is under the few-channel condition.

In this study, we first established a 1024-channel spectrometry system to measure the spectrum by using a mid-energy X-ray, ^{137}Cs and ^{60}Co isotopes as reference radiation fields. The energy ranged from 48 to 1.25 MeV. Nine spectra were measured in the reference radiation fields. The standard values of $H_{\mathrm{p}}(10)$ under each energy condition were recorded as D^j, where j is the number of measured spectra and the maximum value of j is nine. When calculating the value of $H_{\mathrm{p}}(10)$ using the few-channel spectroscopy dose method, the following changes need to be made to Eq. (3) and finally converted to Eq. (4):

$$H_{\mathrm{p}}(10) = \sum_{n=1}^{N} S_n G_n, \quad (4)$$

where N is the number of energy intervals and S_n represents the sum of counts within the energy interval.

Case I If $N = 1$, it is equivalent to the single-channel counting technique, and the threshold voltage corresponding to the low-level discriminator (LLD) of the spectrometry system is used to subtract the baseline noise signal. The value of $H_{\mathrm{p}}(10)$ is calculated using Eq. (5). Since there is only one coefficient G_1, its value can be calibrated directly from the ^{137}Cs isotope reference radiation field. The value of $H_{\mathrm{p}}(10)$ under other energy conditions can be obtained by multiplying the total count value and G_1 using Eq. (5),

$$H_{\mathrm{p}}(10) = S_1 G_1 = \sum_{i=1}^{1024} M_i G_1. \quad (5)$$

Case II If $N = 2$, it is equivalent to the two-channel counting technique, and the value of $H_{\mathrm{p}}(10)$ is calculated using Eq. (6). Unlike the multichannel spectroscopy, the channel number of the two-channel counting technique can be any of the values in the full spectrum. This means that the channel number can be any value between 1 and 1024. The range of the channel numbers corresponding to the energy interval one is $[1, a]$, and the range of the channel numbers corresponding to the energy interval two is $[a + 1, 1024]$,

$$H_{\mathrm{p}}(10) = S_1 G_1 + S_2 G_2 = \sum_{i=1}^{a} M_i G_1 + \sum_{i=a+1}^{1024} M_i G_2. \quad (6)$$

Case III If $N = 3$, it is equivalent to the three-channel counting technique, and the value of $H_{\mathrm{p}}(10)$ is calculated using Eq. (7). The channel number corresponding to the energy interval one is $[1, a]$, the channel number corresponding to the energy interval two is $[a + 1, b]$, and the channel number corresponding to the energy interval three is $[b + 1, 1024]$,

$$H_p(10) = S_1G_1 + S_2G_2 + S_3G_3 = \sum_{i=1}^{a} M_iG_1 + \sum_{i=a+1}^{b} M_iG_2 + \sum_{i=b+1}^{1024} M_iG_3. \quad (7)$$

In Eq. (7), a and b are the channel numbers, ranging from one to 1024. G_1, G_2, G_3 are the counts-to-dose conversion factors (μSv/h/CPS). The established objective equation using the enumeration algorithm is shown in Eq. (8). Among them, $H_p^j(10)$ represents the measured dose value under the jth energy condition, $H_p^8(10)$ represents the measured dose value under ^{137}Cs. The minimum value of the PER under the different a, b, and G values can be found by Eq. (8) (normalized to ^{137}Cs),

$$\arg \text{Min } |(H_p^j(10)/H_p^8(10) - 1). \quad (8)$$

Equation (8) is a function related to the parameters of a, b, and G. The optimal PER for the different a, b, and G values can be found by the enumeration algorithm in Fig. 1. To shorten the search time, the G value is constrained by experience. The range of G is 0–5, and the step width is 0.001. Nine standard measured spectra were used to calculate the values of $H_p(10)$ by the MATLAB software. The program recorded the G, a, and b values at the optimal PER.

When compared with the Monte Carlo simulation and numerical calculation techniques, the enumeration algorithm has the characteristics of being simple and easy to use, with no need to build the detector model, and provides accurate calculation. Figure 1 shows the flowchart using the MATLAB software when N is equal to three, with the flowchart of $N = 2$ being similar to that of $N = 3$.

Owing to the statement formatting requirements of the MATLAB software, a part of the notation in Fig. 1 is different from what is described in Sects. 2.1 and 2.2. $H_p^{10}(j)$ in Fig. 1 is denoted as $H_p^j(10)$, and $H_p^{10}(8)$ in Fig. 1

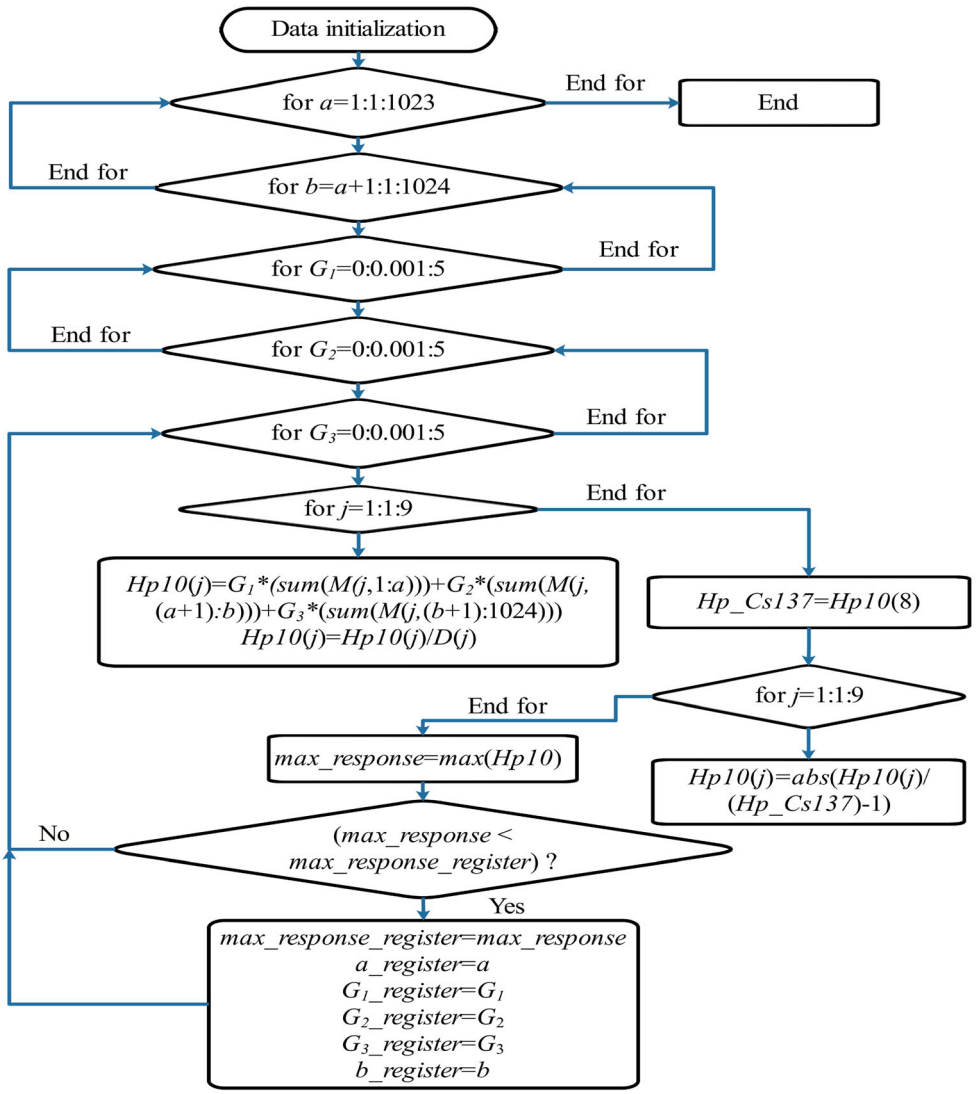

Fig. 1 Software flowchart using enumeration algorithm ($N = 3$) to solve the relevant parameters

is denoted as $H_p^8(10)$. Through the implementation of the flowchart program, the PER optimal values were finally determined and were placed in the *max_response_register*; the optimal G value was placed in G_1*_register*, G_2*_register,* and G_3*_register*, and the a and b values were placed in *a_register* and *b_register*, respectively.

3 Irradiations and testing platform

3.1 Irradiations

The N-60, N-80, N-100, N-120, N-150, N-200, and N-250 narrow-spectrum radiation fields recommended by international standard ISO 4037-1:1996 were established using a mid-energy X-ray machine (model: GX320) [20]. The high-energy radiation field was established by the ^{137}Cs and ^{60}Co isotopes. The energy range of the radiation fields is between 48 keV and 1.25 MeV. The standard instrument used for radiation field measurements is a 1-L spherical ionization chamber (type32002) from PTW. The measurement quantity of the PTW spherical ionization chamber is air kerma (Gy), which can be converted to Sv through the conversion coefficient (Sv/Gy) [21], as shown in Table 1. The conversion factors are derived from the data in international standard ISO 4037-3:1999 multiplied by the calibration factor of the spherical ionization chamber at the national institute of metrology. Since the detector module is used for the measurement of $H_p(10)$, the response as a function of photon energy should be measured on a phantom according to international standard ISO 4037-3:1999. The outer dimensions of phantom with polymethyl methacrylate (PMMA) walls (front wall 2.5 mm thick, other walls 10 mm thick) filled with water are 300 mm × 300 mm × 150 mm [21]. The phantom placed behind the detector module in the reference radiation fields is used to replace the human body for measuring the value of $H_p(10)$. Meanwhile, the build-up layer of the PMMA plate according to international standard ISO 4037-3:1999 is not used because the front end of the detector is covered by the 2-mm Al metal and silicon oxide materials, the Au electrode, and the Si dead layer.

3.2 Spectrum measurement system

Figure 2a shows the structure of the spectrum measurement system using a 4.5 mm × 4.0 mm × 1.2 mm Si-PIN photodetector (model BPW 34) produced by OSRAM Opto Semiconductors. The photosensitive area of the detector is 2.65 mm × 2.65 mm. The detector module includes the Al metal filter material, a Si-PIN photodetector, a charge-sensitive preamplifier, a pole-zero cancellation circuit, and an active filter using operational amplifiers. The X- or gamma rays interact with the Si material in the sensitive layer of the Si-PIN photodetector to generate secondary electrons through the photoelectric effect, Compton effect, and electron pair effect, which in turn generate electron–hole pairs. A current pulse is formed from the electron–hole pairs under the electrical field when a bias voltage is supplied [22]. The current signal is converted into a voltage pulse signal by a charge-sensitive amplifier [3, 4]. The X- or gamma rays detected by the Si-PIN photodetector are amplified into a 1 ~ 2 μs pulse signal, and the theoretical upper limit of linearity can be up to 500,000 counts per second (CPS). The EPD first counts the number of electrical pulses and then calls the counts-to-dose conversion factors to calculate the value of $H_p(10)$ for X- and gamma radiation. The volume of the Al shell of the detection module unit is 117 mm × 47 mm × 17 mm. The nuclear pulse signal generated by the detector module

Table 1 Radiation qualities used in radiation protection

Tube voltage (kV)	Tube current (mA)	HVL (mm Cu)	Distance (m)	Mean energy (keV)	Conversion factor (Sv/Gy)	Standard value (μSv/h)
Narrow spectrum						
60	1.76	0.24	3.0	47.9	1.69	3905
80	1.05	0.58	3.0	65.0	1.84	4024
100	0.88	1.11	3.0	83.1	1.82	4132
120	0.59	1.73	3.0	100.0	1.76	3826
150	0.99	2.35	3.0	117.7	1.71	13,373
200	0.99	4.01	3.0	164.0	1.62	21,795
250	0.99	5.16	3.0	207.5	1.52	35,969
Isotope source						
	^{137}Cs		1.0	662.0	1.21	998
	^{60}Co		1.0	1250.0	1.16	5000

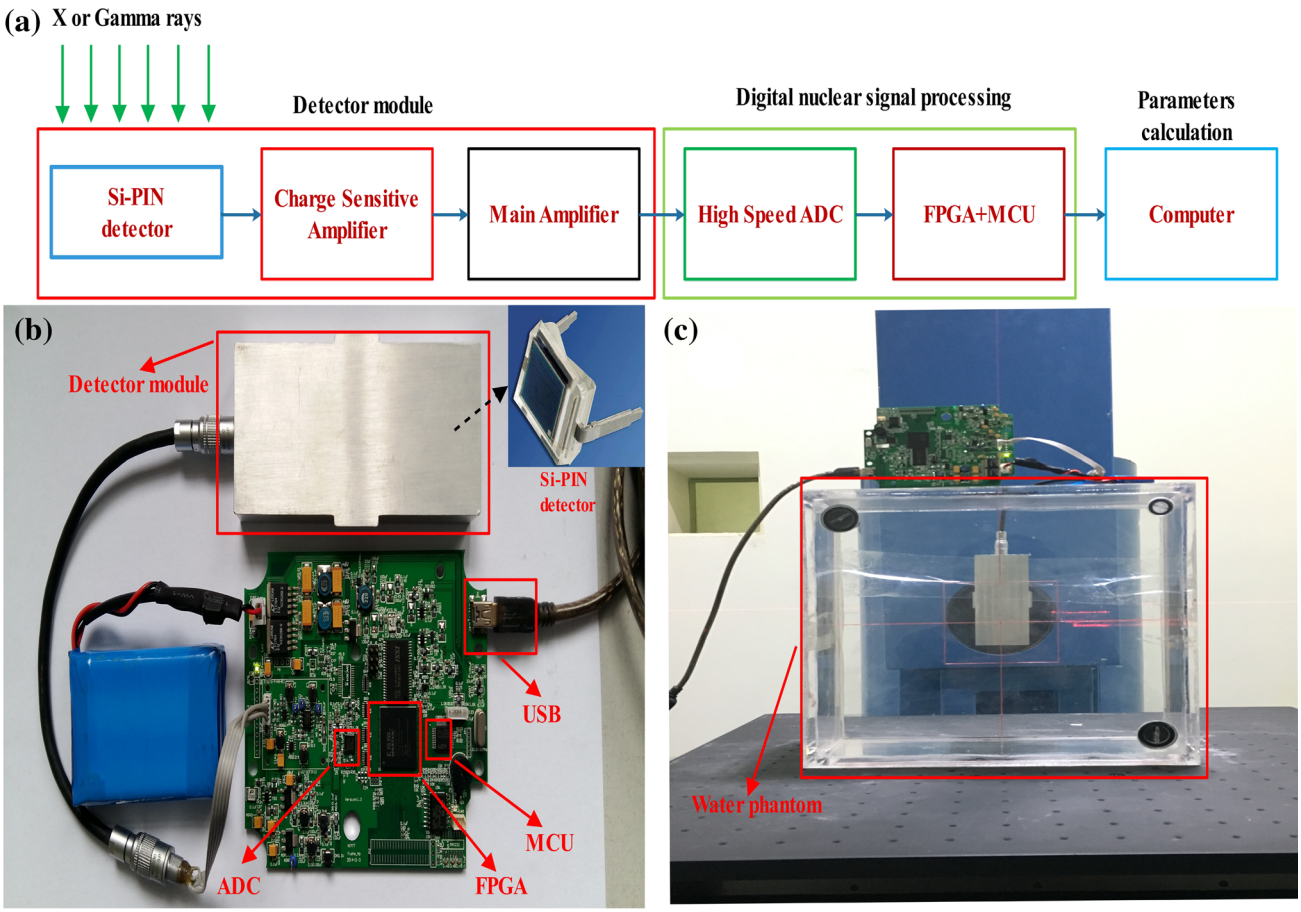

Fig. 2 (Color online) **a** Schematic of the Si-PIN spectrum measurement system; **b** hardware for the Si-PIN spectrum measurement system; and **c** a water phantom was placed behind the detector module

is sampled by a high-speed (40 MSPS) ADC to form multichannel spectrum data through the FPGA. Finally, the spectral data are transmitted through the MCU USB module [23]. Using the computer to calculate the related parameters, the focusing procedure implements the algorithm in Fig. 1 using the MATLAB software. The X- or gamma rays are filtered through the shielding Al material and then detected by the Si-PIN photodetector.

Figure 2b shows the hardware implementation of the Si-PIN photodetector. The detector module uses the Al material for protection against light and electromagnetic interference. Additionally, the Al material is used as the front-end filter material of the Si-PIN photodetector to compensate the PER. The digital processing of the nuclear pulse signal by the FPGA uses the trapezoidal pulse shaping technique [24, 25].

The Si-PIN photodetector is generally composed of SO_2 material, the Al electrode, the dead layer, and the sensitive layer. The insulating layer has an important influence on low-energy (< 20 keV) radiation detection, but the attenuation effect is relatively small for X/γ rays above 48 keV. Because the detector datasheet used in the study did not give the size value of the above materials, the detector calibration is performed in the standard radiation field to avoid the error caused by building the detector model using the Monte Carlo method.

The cathode of the Si-PIN photodetector is connected to a + 5 V direct current (DC) voltage through a 100 M bias resistor (anode ground), in addition to a charge-sensitive amplifier through capacitive coupling. When using a low-power charge-sensitive amplifier and main amplifier, the power consumption of the above circuit is about 1 mW.

To improve the measurement accuracy of the Si-PIN photodetector under the different photon energies, we first use the Al metal material to achieve the initial correction of the PER. Next, the nuclear pulse signals detected by the Si-PIN photodetector are collected by the back-end electronics, and the PER is corrected by software. Differences from the references are: (1) The front-end filter material of the Si-PIN photodetector uses the Al metal material to attenuate the radiation; compared with using Cu, Sn, and other materials to compensate for the PER, this method has a simple structure and is easy to implement; (2) the bias voltage of the Si-PIN photodetector is 5 V, which is low

power consumption and of more practical value; (3) by measuring the standard spectrum instead of the Monte Carlo simulation technique to solve the counts-to-dose conversion factors, the calculation error caused by the inaccuracy of constructing the detector model is reduced and the measuring accuracy is further improved [17, 18].

To obtain the optimal PER, a 1024-channel digital spectrometer based on a Si-PIN photodetector was established in this study. Testing scenes of the Si-PIN photodetector spectrum system in the reference radiation fields are shown in Fig. 2c. The detector module was placed in front of a water phantom, and the Si-PIN photodetector was coincident with the center of the radiation fields by a laser-positioning device.

When the above measurement system is fully prepared, the following procedures are used to implement acquisition and analysis of the spectral data. First, the system measures the full spectrum of a known standard dose value in the reference radiation fields. Second, the enumeration algorithm is used to find out the optimal PER under the conditions of two and three energy intervals. Finally, the channel number and the counts-to-dose conversion factors corresponding to the optimal PER were recorded. Compared with the average channel number distribution of the multichannel spectroscopy, the channel number corresponding to the energy intervals in the few-channel spectroscopy dose method can be any of the channels. The channel number and the counts-to-dose conversion factors under the optimum PER can be applied in the EPD design.

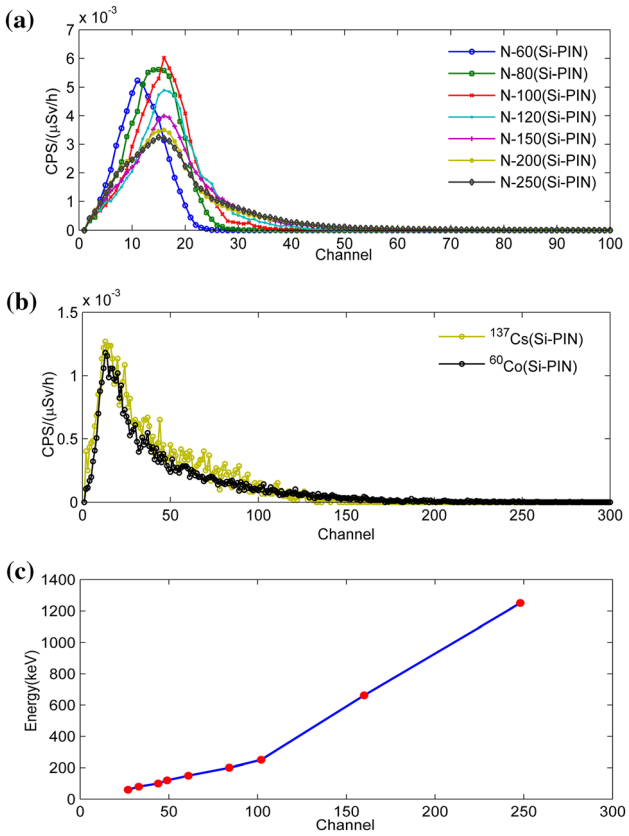

Fig. 3 (Color online) **a** Measured spectrum of the Si-PIN photodetector under the narrow-spectrum series; **b** measured spectrum of the Si-PIN photodetector at the ^{137}Cs and ^{60}Co isotopes; and **c** energy-scale curve for the Si-PIN photodetector

4 Experimental results and discussion

Figure 3a shows the energy spectrum of the Si-PIN photodetector measured with the N-series narrow spectrum in the reference radiation fields recommended by international standard ISO 4037-1:1996. The spectrum measurement time is 60 s. The abscissa in Fig. 3a is the channel number, and the ordinate is the measured counts value divided by the standard dose rate value.

Figure 3b shows the energy spectrum of the Si-PIN photodetector measured in the ^{137}Cs and ^{60}Co isotope reference radiation fields. The spectrum measurement time is 60 s. As shown in Fig. 3b, the measured spectrum of the ^{137}Cs and ^{60}Co isotopes has no characteristic energy peak, and both spectra at the low-energy section are overlapped. The measured spectrum of ^{60}Co has more counts in the high-energy part than that of ^{137}Cs, but there is no linear relationship between the channel number and the energy.

Figure 3a, b shows that the energy deposition in the Si-PIN photodetector is most concentrated on the low-energy section. The reason is that the sensitive layer thickness of the Si-PIN photodetector is about 100 μm, most of the high-energy rays pass directly through the detector, and only a small part of the energy is accumulated by the Compton effect.

The end-point energy of the spectrum produced by an X-ray machine is equal to the tube voltage (kV). Figure 3c is derived from the energy scaling based on the measured spectrum at the mid-energy X-ray machine, ^{137}Cs and ^{60}Co isotope radiation fields. The procedure for the determination of the abscissa point of the spectrum reaching the channel axis is through the linear regression model applied to the end section of the measured spectrum in the reference radiation fields [26]. For ^{137}Cs and ^{60}Co isotopes, the energy detected by the detector is smaller than the incident gamma rays, and the end-point energy corresponds to 662 keV and 1250 keV, respectively. Figure 3c is plotted by the corresponding channel number and the end-point energy found in Fig. 3a, b. As shown in Fig. 3c, the channel number and energy were linear in the energy range from 60 to 250 keV. However, as the particle energy increases, the energy linearity of the Si-PIN photodetector decreases. The reason is that with the increase in energy, the energy deposition on the Si-PIN photodetector is

mainly caused by the Compton effect, and the high-energy rays cannot completely be absorbed by the photoelectric effect.

By measuring the spectral data of Fig. 3a, b in the reference radiation fields, we can use the MATLAB to write the flowchart software in Fig. 1 to calculate the relevant parameters.

When $N = 1$, it is equivalent to calculating the dose rate value by the single-channel counting technique. G_1 can be directly calculated for the ^{137}Cs isotope radiation field. The PER at $N = 1$, 2, and 3 are shown in Table 2.

When $N = 1$, the parameter is calculated as $G_1 = 0.337$. When $N = 2$, the relevant parameters are calculated as $a = 107$, $G_1 = 0.260$, and $G_2 = 2.403$. When $N = 3$, the related parameters are calculated as $a = 5$, $b = 96$, $G_1 = 2.269$, $G_2 = 0.155$, and $G_3 = 2.166$.

Figure 4 shows the optimal PER with $N = 1$, 2, and 3. As can be seen from Fig. 4, as N increases, the PER decreases from ± 48 to ± 2%. In this study, we propose to use the two and three energy intervals to further improve the PER of the Si-PIN photodetector. The few-channel spectroscopy dose method meets the requirements of low power consumption, low cost, and accurate measurement. The relevant parameter values can be applied in the EPD design through the ultra-low-power MCU.

The enumeration algorithm needs to convert the a and b values into useful threshold voltage values. The input voltage range is 0–4 V, and each channel corresponding to voltage value is 4 mV under the condition of 1024 channels. The noise voltage threshold is controlled at 50 mV. When $N = 2$, the corresponding threshold voltage is 50 mV and 0.42 V, respectively. When $N = 3$, the corresponding threshold voltage is 50 mV, 70 mV, and 0.43 V, respectively. In the later EPD design, the appropriate threshold values can be selected according to the internal counter number of the ultra-low-power MCU.

The PER according to IEC 61526:2010 allows − 29–+67% plus the expanded relative uncertainty (less than 10%) of the conventional quantity value of the personal dose equivalent, $H_p(10)$, which for the reference radiation

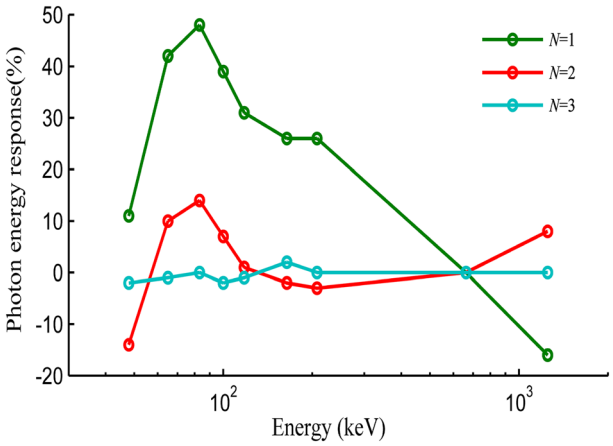

Fig. 4 (Color online) Optimal PER curve under $N = 1$, 2, and 3

fields of radiation protection qualities used is 5.0% ($k = 2$). The influences in the measurement of $H_p(10)$ mainly include conventional quantity value, repeatability, dose rate nonlinear, energy response, and angular response [19, 27].

Since the measurement process was carried out under the medium radiation intensity of 1 ~ 36 mSv/h and the measurement time is 60 s, the uncertainty caused by repeatability and nonlinear dose rate was small compared with the uncertainty of the conventional quantity value. When the PER is equal to ± 14% and ± 2%, the relative standard uncertainties calculated according to uniform distribution are 8.1% and 1.2%, respectively. The expanded relative uncertainty ($k = 2$) for the measurement of $H_p(10)$ without considering other angular responses is 16.9% and 5.5% under the condition of two and three energy intervals.

5 Conclusion

In this study, we established a spectrum measurement system based on a Si-PIN photodetector and performed full-spectrum measurement in the reference radiation fields

Table 2 PER at $N = 1$, 2, and 3

Mean energy (keV)	47.9	65.0	83.1	100.0	117.7	164.0	207.5	662.0	1250.0
Standard value (μSv/h)	3905	4024	4132	3826	13,373	21,795	35,969	998	5000
Measured value (μSv/h), $N = 1$	4347	5727	6113	5302	17,547	27,568	45,197	998	4202
Photon energy response (%), $N = 1$	11	42	48	39	31	26	26	0	−16
Measured value (μSv/h), $N = 2$	3359	4415	4709	4084	13,531	21,254	34,860	998	5404
Photon energy response (%), $N = 2$	− 14	10	14	7	1	− 2	− 3	0	8
Measured value (μSv/h), $N = 3$	3828	3975	4112	3749	13,193	22,200	35,971	998	4996
Photon energy response (%), $N = 3$	− 2	− 1	0	− 2	− 1	2	0	0	0

used for radiation protection. Instead of using the Monte Carlo simulation technique or numerical calculation techniques to solve the G function, we used the enumeration algorithm to find the optimal PER under the few-channel spectroscopy condition. According to the requirements of IEC 61526:2010, the optimal PER at 0° angle of radiation incidence can be controlled within± 14% and ± 2% in the range of 48 keV to 1.25 MeV under the conditions of two and three energy intervals, respectively.

For future work, the threshold voltage values solved by the enumeration algorithm will be adopted in EPD development. After the EPD completes parameter migration and instrument design, other technical parameters such as angular response, inherent error, and high nonlinear dose rate will be systematically tested in the reference radiation fields used for radiation protection. Our future plans include: (1) using the non-extended dead time model to improve the nonlinearity problem at a high dose rate; (2) establishing the reference radiation fields below N-60; and (3) using two Si-PIN photodetectors to measure the personal dose equivalent in a wide energy range.

References

1. C. Hranitzky, H. Stadtmann, Simulated and measured $H_p(10)$ response of the personal dosemeter Seibersdorf. Radiat. Prot. Dosim. **125**, 166–169 (2007). https://doi.org/10.1093/rpd/ncm336
2. T. Bolognese-Milsztajn, M. Ginjaume, M. Luszik-Bhadra et al., Active personal dosemeters for individual monitoring and other new developments. Radiat. Prot. Dosim. **112**, 141–168 (2004). https://doi.org/10.1093/rpd/nch286
3. T. Nakamura, M. Sasaki, O. Ueda et al., Characterisation of a real-time personal neutron dosemeter with two silicon detectors. Radiat. Prot. Dosim. **85**, 45–48 (1999). https://doi.org/10.1093/oxfordjournals.rpd.a032894
4. M. Takahashi, M. Sekiguchi, H. Miyauchi et al., Performance of the $H_p(10)$ and $H_p(0.07)$ measurable electronic pocket dosimeter for gamma-and beta-rays. J. Nucl. Sci. Technol. **45**, 225–228 (2008). https://doi.org/10.1080/00223131.2008.10875828
5. T. Nunomiya, S. Abe, I. Matsumoto et al., Development of new generation-type multi-functional electronic personal dosemeters. J. Nucl. Sci. Technol. **45**, 175–178 (2008). https://doi.org/10.1080/00223131.2008.10875815
6. T. Nunomiya, S. Abe, K. Aoyama et al., Development of advanced-type multi-functional electronic personal dosemeter. Radiat. Prot. Dosim. **126**, 284–287 (2007). https://doi.org/10.1093/rpd/ncm059
7. H.H. Tseng, H.F. Chang, Energy compensation characteristics of Cu and Sn on low cost Si photodiodes for gamma (Aleph) dosimetry applications. IEEE. T. Nucl. Sci. **39**, 1523–1527 (1992). https://doi.org/10.1109/23.173237
8. C.R. Chen, S.H. Jiang, H.H. Tseng et al., Energy response and filter compensation of PIN Si photodiode for personal dosimetry application. IEEE. T. Nucl. Sci. **40**, 857–862 (1993). https://doi.org/10.1109/23.256674
9. H. Dombrowski, Area dose rate values derived from NaI or LaBr 3 spectra. Radiat. Prot. Dosim. **160**, 269–276 (2014). https://doi.org/10.1093/rpd/nct349
10. S. Tsuda, T. Yoshida, M. Tsutsumi et al., Characteristics and verification of a car-borne survey system for dose rates in air: KURAMA-II. J. Environ. Radioactiv. **139**, 260–265 (2015). https://doi.org/10.1016/j.jenvrad.2014.02.028
11. Y.Y. Ji, D.S. Hong, T.K. Kim et al., Application of the dose conversion factor for a NaI (Tl) detector to the radwaste drum assay. Radiat. Meas. **46**, 503–509 (2011). https://doi.org/10.1016/j.radmeas.2011.03.021
12. J.I. Young-Yong, K.H. Chung, C.J. Kim et al., Application of the dose rate spectroscopy to the dose-to-curie conversion method using a NaI (Tl) detector. Radiat. Phys. Chem. **106**, 320–326 (2015). https://doi.org/10.1016/j.radphyschem.2014.08.009
13. A. Clouvas, S. Xanthos, M. Antonopoulos-Domis et al., Monte Carlo based method for conversion of in situ gamma ray spectra obtained with a portable Ge detector to an incident photon flux energy distribution. Health Phys. **74**, 216–230 (1998). https://doi.org/10.1097/00004032-199802000-00007
14. M. Reginatto, Overview of spectral unfolding techniques and uncertainty estimation. Radiat. Meas. **45**, 1323–1329 (2010). https://doi.org/10.1016/j.radmeas.2010.06.016
15. H.Z. Dizaji, T. Kakavand, F.A. Davani, Spectrometry and dosimetry of fast neutrons using pin diode detectors. Nucl. Instrum. Meth. A. **741**, 84–87 (2014). https://doi.org/10.1016/j.nima.2013.12.018
16. L.S.R. Oliveira, C.C. Conti, A.S. Amorim et al., NaI (Tl) scintillator detectors stripping procedure for air kerma measurements of diagnostic X-ray beams. Nucl. Instrum. Meth. A. **705**, 106–110 (2013). https://doi.org/10.1016/j.nima.2012.12.002
17. H.Z. Dizaji, Energy response improvement for photon dosimetry using pulse analysis. Chin. Phys. C. **40**, 026203 (2016). https://doi.org/10.1088/1674-1137/40/2/026203
18. Y. Lotfi, H.Z. Dizaji, F.A. Davani, Detection and dosimetry studies on the response of silicon diodes to an ^{241}Am-Be source. Jinst. **9**, P06023 (2014). https://doi.org/10.1088/1748-0221/9/06/P06023
19. IEC 61526, Radiation protection instrumentation—measurement of personal dose equivalents $H_p(10)$ and $H_p(0.07)$ for X, gamma, neutron and beta radiations—direct reading personal dose equivalent meters. International Electrotechnical Comission (2010)
20. ISO 4037-1, X and gamma reference radiation for calibrating dosemeters and dose rate meters and for determining their response as a function of photon energy—part 1: radiation characteristics and production methods. International Organization for Standardization (1996)
21. ISO 4037-3, X and gamma reference radiation for calibrating dosemeters and doserate meters and for determining their response as a function of photon energy—part 3: calibration of area and personal dosemeters and the measurement of their response as a function of energy and angle of incidence. International Organization for Standardization (1999)
22. S.S. Qu, Z. Guo, R.Z. Tai et al., Design of soft X-ray photon correlation spectroscopy device. Nucl. Tech. **42**, 040103 (2019). https://doi.org/10.11889/j.0253-3219.2019.hjs.42.040103. **(in Chinese)**
23. Y. Yuan, L.Q. Zhang, X.L. Luo, A real-time peak detection method for nuclear pulse signal and energy spectrum analysis. Nucl Tech **42**, 020404 (2019). https://doi.org/10.11889/j.0253-3219.2019.hjs.42.020404 **(in Chinese)**
24. J. Lanchares, O. Garnica, J.L. Risco-Martín et al., Real-time evolvable pulse shaper for radiation measurements. Nucl. Instrum. Meth. A. **727**, 73–83 (2013). https://doi.org/10.1016/j.nima.2013.05.164
25. D. Alberto, M.P. Bussa, E. Falletti et al., Digital filtering for noise reduction in nuclear detectors. Nucl. Instrum. Meth. A. **594**, 382–388 (2008). https://doi.org/10.1016/j.nima.2008.06.032

26. R. Künzel, S.B. Herdade, R.A. Terini et al., X-ray spectroscopy in mammography with a silicon PIN photodiode with application to the measurement of tube voltage: X-ray spectroscopy in mammography with a silicon photodiode. Med. Phys. **31**, 2996–3003 (2004). https://doi.org/10.1118/1.1803432

27. J. Cardoso, J.A.M. Santos, L. Santos et al., Characterization of an active dosemeter according to IEC 61526: 2010. Radiat. Prot. Dosim. **170**, 127–131 (2016). https://doi.org/10.1093/rpd/ncw090